Molecular Crystals and Liquid Crystals

Publication details, including instructions for authors and subscription information:
http://www.tandfonline.com/loi/gmcl20

The Origin of High Optical Tilt in a Homologous Series of Fluorinated Antiferroelectric Liquid Crystals

W. Piecek [a], Z. Raszewski [a], P. Perkowski [a], J. Kędzierski [a], J. Rutkowska [a], J. Zieliński [a], E. Nowinowski-Kruszelnicki [a], R. Dąbrowski [b], M. Tykarska [b] & J. Przedmojski [c]

[a] Institute of Applied Physics, Military University of Technology, Warsaw, Poland

[b] Institute of Chemistry, Military University of Technology, Warsaw, Poland

[c] Faculty of Physics, Warsaw University of Technology, Warsaw, Poland

Version of record first published: 31 Aug 2006

To cite this article: W. Piecek, Z. Raszewski, P. Perkowski, J. Kędzierski, J. Rutkowska, J. Zieliński, E. Nowinowski-Kruszelnicki, R. Dąbrowski, M. Tykarska & J. Przedmojski (2005): The Origin of High Optical Tilt in a Homologous Series of Fluorinated Antiferroelectric Liquid Crystals, Molecular Crystals and Liquid Crystals, 436:1, 149/[1103]-165/[1119]

To link to this article: http://dx.doi.org/10.1080/15421400590955578

Mol. Cryst. Liq. Cryst., Vol. 436, pp. 149/[1103]–165/[1119], 2005

ISSN: 1542-1406 print/1563-5287 online
DOI: 10.1080/15421400590955578

Taylor & Francis
Taylor & Francis Group

The Origin of High Optical Tilt in a Homologous Series of Fluorinated Antiferroelectric Liquid Crystals

W. Piecek
Z. Raszewski
P. Perkowski
J. Kędzierski
J. Rutkowska
J. Zieliński
E. Nowinowski-Kruszelnicki
Institute of Applied Physics, Military University of Technology, Warsaw, Poland

R. Dąbrowski
M. Tykarska
Institute of Chemistry, Military University of Technology, Warsaw, Poland

J. Przedmojski
Faculty of Physics, Warsaw University of Technology, Warsaw, Poland

The compounds from the fluorinated nF6B (n = 1,2,3,4,5,6,7) homologous series were investigated by means of optical, electrooptical, refractometrical, dielectric, densytometric, X-ray and IR spectroscopy methods. For some compounds being a subject of investigations a computer simulation of molecular properties were done. In our opinion high value of optical tilt θ_o angle in comparison with a tilt angle obtained from X-ray measurements can be interpreted in terms of de Vries model of SmA* phases as well as of dimers creation process.

Keywords: antiferroelectric liquid crystals; ferroelectric liquid crystals; helical pitch; layer spacing; orthoconic antiferroelectric liquid crystals; refractive indices; spontaneous polarisation; tilt angle

This work was supported by the Polish Ministry of Scientific Research and Information Technology in years 2003–2006 (grant No. 0 T00C 006 25).

Address correspondence to Wiktor Piecek, Institute of Applied Physics, Military University of Technology, Kaliskiego Str. 2, 00-908 Warsaw, Poland. E-mail: wpiecek@wat.edu.pl

1. INTRODUCTION

Since the discovery of the ferroelectric SmC^* [1] and antiferroelectric SmC_A^* [2] phases, a variety of theoretical and experimental investigations were performed, in order to understand the origin and the nature of their optical tilt angle.

In the last few years one can notice some interesting antiferroelectric liquid crystals (AFLC) with high optical tilts [3–5].

AFLC with the tilt angle of 45° (so called orthoconic antiferroelectric liquid crystals–OAFLCs) produces optically negative and uniaxial cell with the optic axis perpendicular to the cell surface. Such a cell placed between two crossed polarizers exhibits the perfect dark state (without any light leakage). What is more, the quality of the black state does not depend on the alignment uniformity of smectic layers with respect to polarizer direction. After switching to the first of two ferroelectric states, the optic axis of AFLC rotates by 90 degrees and assumes a uniplanar position to cell electrodes. If this optic axis between two crossed polarizers is accurately adjusted the polarization plane of the normally incident light rotates by 90 degrees hence, the optimum transmission (bright state) is obtained. Such alignment of the sample can easily be achieved with standard procedures which are widely used in twisted nematic (TN) and supertwisted nematic (STN) technologies. So, using OAFLC and near standard liquid crystal technologies one can realise not very expensive AFLC display with rather high quality. For this reason one can notice a big interest in developing OAFLC materials [3–12], which are absolutely necessary for working out different kinds of OAFLC displays (OAFLCD). To develop the technology of OAFLCDs the origin of the very high optical tilt θ_o in AFLC should be known.

In this paper, we intend to present our point of view on this subject and discuss it on the basis of our experimental results.

2. EXPERIMENTAL, RESULTS AND DISCUSSION

It has been found [9] that high tilted materials without pretransitional effects [5,13] are created within the compounds from the homologous series of: biphenyl benzoates with molecular structure presented below:

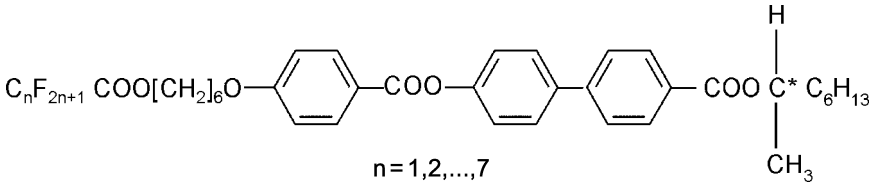

These materials have been further called in short nF6B series.

Table 1 consists of transition temperatures and enthalpies for nF6B series. The phase transition temperatures and enthalpies were determined by differential scanning calorimetry (DSC), using the SETARAM 141 calorimeter. Phase transition temperatures and phase textures were observed also using polarising optical microscope BIOLAR PI equipped with the LINKAM 660 hot stage, controlled by the TMS 93 unit.

The compounds from the nF6B homologous series were investigated by means of optical, electrooptical, refractometrical, dielectric, densytometric, X-ray and IR spectroscopy methods. All measurements were done during cooling from isotropic phases with the cooling rate around 0.01 deg/min.

To compare some results obtained for fluorinated nF6B series, some compounds from fluorinated nF6Bi (2) homologous series and non-fluorinated nH6B (3) one with structural formulas presented below were also investigated.

TABLE 1 Transitions Temperatures T_D [°C] and Enthalpies ΔH [kJ/mol] Determined by DSC and Transition Temperatures T_M [°C] Determined by Optical Microscopy for the Fluorinated Compounds of nF6B Series

n	nF6B	Cr	SmC_A^*	SmC^*	SmA^*	Iso
1	1F6B	40.1	71.3	107.2	112.5	T_D
		33.203	0.002	1.214	3.308	ΔH
		34.5	72.4	107.5	113.0	T_M
2	2F6B	30.8	91.5	110.0	113.5	T_D
		10.886	0.054	0.004	4.313	ΔH
		32.2	92.1	111.0	115.1	T_M
3	3F6B	18.5	98.0	113.2	119.2	T_D
		12.002	0.667	1.047	4.438	ΔH
		17.0	99.1	115.3	120.7	T_M
4	4F6B	31.0	102.3	121.8	124.3	T_D
		26.253	0.042	1.597	3.350	ΔH
		33.0	107.3	122.7	125.3	T_M
5	5F6B	39.3	102.3	125.8	131.3	T_D
		26.169	0.042	1.382	3.936	ΔH
		37.0	103.5	126.4	133.0	T_M
6	6F6B	43.0	115.7	125.0	130.6	T_D
		24.368	0.004	0.293	5.820	ΔH
		42.1	117.4	127.10	132.5	T_M
7	7F6B	33.8	115.0	131.6	143.4	T_D
		17.502	0.008	0.461	5.192	ΔH
		32.0	108.9	139.2	144.8	T_M

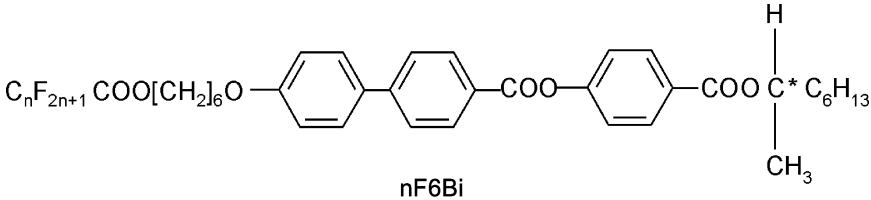

nF6Bi

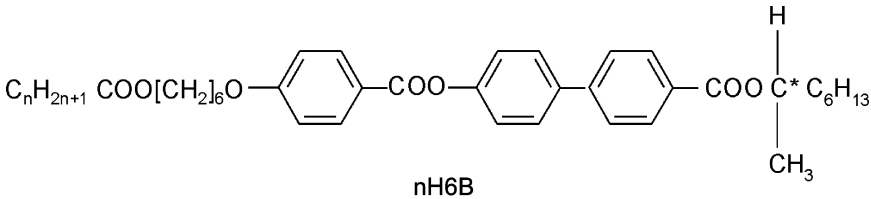

nH6B

2.1. Tilt Angle

Tilt angle θ_0 was studied by means of optical switching angle measurements. These electrooptical studies were done using cells in the form of flat capacitors intentionally prepared in our laboratory. Cells were assembled using flat glass for TN technology. The glass was coated with indium tin oxide layer in the form of electrodes. The thickness of cells varied between 1.5 and 2.5 μm. In order to achieve a uniform bookshelf geometry of samples, the electrodes were usually coated with about 300 angstroms of different kinds of polyimides and polyamides (nylons) followed by suitable rubbing. Cells were filled with the material under study in isotropic phase and then samples were slowly cooled from the isotropic to the SmA^* phase in the presence of low frequency (15 Hz) electric field ($E = 5\,V/\mu m$). Results of these measurements are shown in the Figure 1.

As it can easily be seen in the Figure 1 that the optical tilt angles (measured at $E = 5\,V/\mu m$) for compounds from nF6B series with n = 1,2,3,4 and 5 differ much in the character from compounds with n = 6 and 7. Optical tilt angles for n = 1,2,3,4 and 5 are higher then for n = 6 and 7 ones, and show quick saturation, while the compounds with n = 6 and 7 show no sign of saturation when the temperature T decreases. It is worth pointing out that the magnitudes of optical tilts for compounds with n = 1,2,3,4, and 5 significantly jump at the phase transitions from SmA^* to SmC^* while for n = 6 and 7 ones, remain continuous at this transitions.

Generally speaking, one can notice, that the optical tilt angles for nF6B compounds are much higher than for nH6B [16] and comparable with nF6Bi ones.

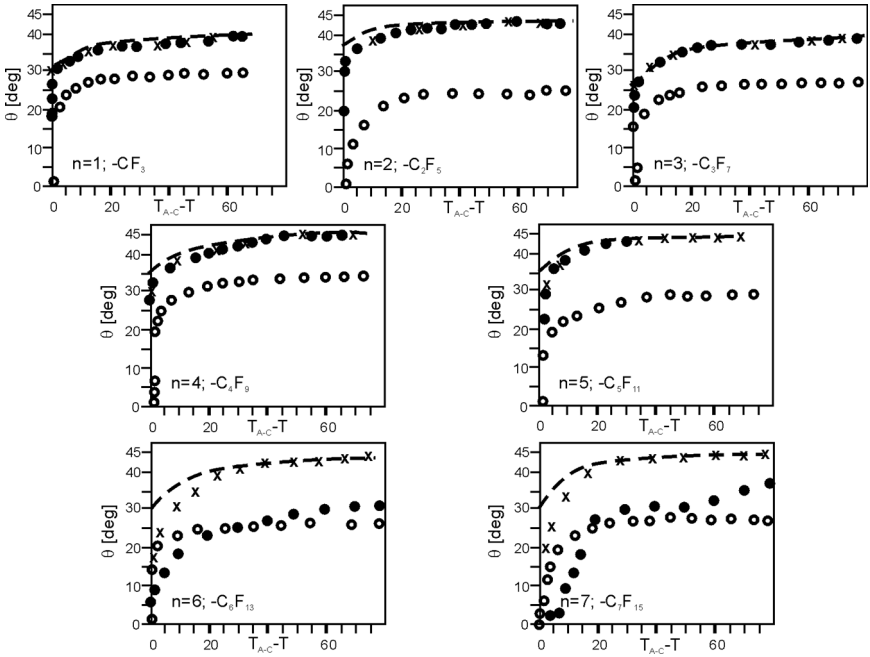

FIGURE 1 The tilt angle θ as a function of relative temperature $T_{AC} - T$ plotted for nF6B series with n = 1,2,...,7 carbon atoms in fluorinated chain $C_nF_{2n+1;}$ (●) optical tilt θ_o obtained from electrooptical measurements with electrodes covered with nylon, $E = 5\,V/\mu m$; (x) optical tilt θ_o obtained from electrooptical measurements with electrodes covered with polyimide, $E = 25\,V/\mu m$; empty circles (○) denote results obtained from X-ray measurements (calculated as: $\theta_x = \text{acos}(d/d_A)$ where: d is a layer spacing in SmC^* or SmC_A^*, d_A is a layer spacing in SmA^* phase); dashed lines (—) denote results calculated as: acos (d/L) where L is a length of an aggregate consisting of two antiparallely oriented molecules (see Table 2).

2.2. X-ray Diffraction Measurement

The smectic layer thicknesses as a function of temperature were studied by small-angle X-ray scattering (SAXS) experiments. All measurements were done using X'Pert powder diffractometer with Cu lamp, Ni filter and proportional counter. The sample was placed in thermo-stabilised chamber driven by temperature controller. The sample of AFLC under study was placed (in the solid state) on the bare glass plate and melted into isotropic phase. In this way one surface of AFLC sample leaves free what promoted homeotropic arrangement in the sample due to the surface tension. The internal diffraction maxima

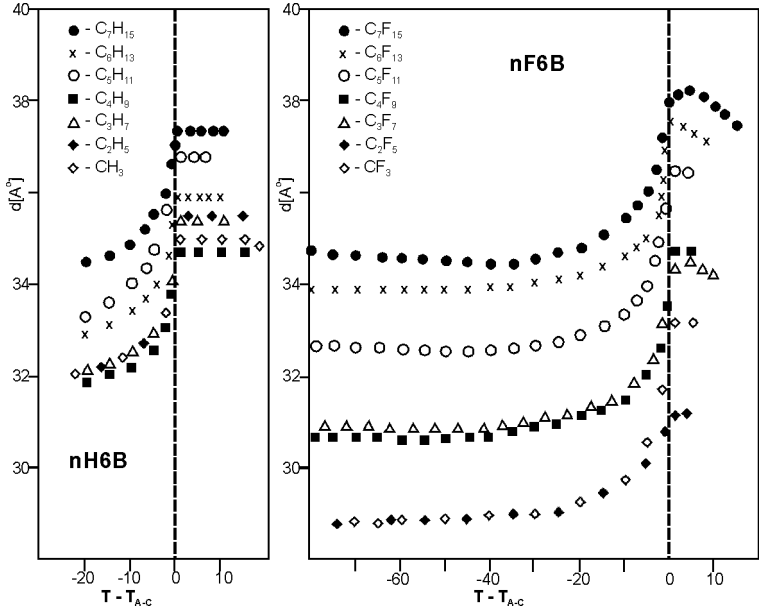

FIGURE 2 The smectic layer thicknesses d and d_A as a function of temperature T for nH6B (left diagram) and nF6B (right diagram).

of SmA*, SmC* and SmC_A* phases were registered for full temperature profiles. These internal diffraction maxima were taken for calculation of smectic layer thicknesses using the Bragg law. Results of X-ray diffraction measurements for fluorinated nF6B series and nonfluorinated nH6B series are plotted in the Figure 2.

Note that the layer spacing d of fluorinated compound 6F6B and 7F6B is higher than for 6H6B and 7H6B while the layer spacing of nF6B compounds with n = 1,2,3,4 and 5 is much smaller than those for their protonated analogs nH6B. If one compares layer spacing d measured by SAXS in SmA* phases for nF6B series (compare left diagram of Figure 2 and Table 2) with the molecular lengths l (or even with the lengths l_m of fully extended molecules), one notices that d are much smaller then l_m. The difference is as much as 8Å high, in the case of 7F6B compound. After a clear increase of d_A on cooling through the SmA* phase, layer thickness d decreases sharply after the transition to the SmC* phases. The maximum decrease of the layer thickness value was observed for 5F6B at 40°C below the SmA* – SmC* transition and was about 5Å. It is worth stressing that while on further cooling d again increases slowly.

TABLE 2 Results of Some Computer Simulation and Experimental Results for nF6B Molecules

nF6B	l [Å]	l_m[Å]	L_1[Å]	L_2[Å]	μ [D]	μ_1[D]	μ_2[D]	d [Å]	d_A[Å]	L_A[Å]	L [Å]	θ_A [deg]	θ [deg]
1F6B	34.8	37.9	35.0	55.0	2.40	1.80	1.80	28.8	33.2	36.8	38.0	25	40
2F6B	36.5	39.1	37.3	58.0	2.47	1.67	1.69	28.9	31.3	38.0	39.8	34	44
3F6B	37.5	40.6	39.6	61.0	2.54	1.54	1.53	30.9	34.5	38.0	40.3	25	39
4F6B	39.1	41.9	41.9	64.0	2.61	1.41	1.39	30.6	34.8	42.0	43.0	34	45
5F6B	40.3	43.3	44.1	67.0	2.68	1.28	1.26	32.5	36.5	44.0	46.0	34	45
6F6B	41.9	44.7	46.4	70.0	2.75	1.14	1.13	34.0	37.6	44.0	47.0	31	44
7F6B	43.1	46.1	49.0	73.0	2.80	1.00	1.00	34.6	38.1	45.5	49.0	33	45

l - Calculated Optimum Molecular Length, l_m - Calculated Length of Fully Extended Molecule, L_1 - Calculated Total Length of Dimer 1, L_2 - Calculated Total Length of Dimer 2, μ - Calculated Total Dipole Moment of Single Isolated Molecule, μ_1 - Calculated Total Dipole Moment of Virtual Dimer 1, μ_2 - Calculated Total Dipole Moment of Virtual Dimer 2, d - Measured by SAXS Layer Spacing of the SmC* Phase at $T - T_{AC} = 60^{\circ}C$, d_A-Measured by SAXS Layer Spacing of the SmA* Phase at $T - T_{AC} = +2^{\circ}C$, L_A - Estimated Average Length of Objects Which Build up the SmA* Phase, L - Estimated Average Length of Objects Which Build up the SmC* Phase at $T - T_{AC} = -60^{\circ}C$, $\theta_A = \text{acos}(d_A/L_A)$ - Calculated Tilt Angle in the de Vrise SmA* Phase, $\theta = \text{acos}\,(d/L)$ - Calculated Tilt Angle in the de SmC* Phase at $T - T_{AC} = 60^{\circ}C$.

Near the same regularity in layer thicknesses observed for nF6B compounds, manifests in nF6Bi series. The d/d_A ratio in both cases strongly depends on the length of the fluorinated unit. The ratio d/d_A is in range [0.91, 0.94] for nF6Bi compound and it is higher than those for nF6B one which is in range [0.87, 0.92]. Moreover, the increase of the layer spacing d upon the temperature decrease for compounds from nF6B homologous series is rather marginally observed while it is rather considerable in case of nF6Bi compounds [9]. Although the layer spacing d of nF6B shrinks, as it has been described above, magnitudes of these changes are not sufficient to fully explain the origin of high optical tilt angle θ_o measured for those compounds. As one can see in the Figure 1 the X-ray tilts θ_x calculated as

$$\theta_x = \text{a}\cos\frac{d}{d_a} \tag{4}$$

are much smaller than θ_o one.

2.3. Helical Pitch

The helical pitch p was investigated on the base of the phenomenon of selective reflections of the light. When the light incidents normally to

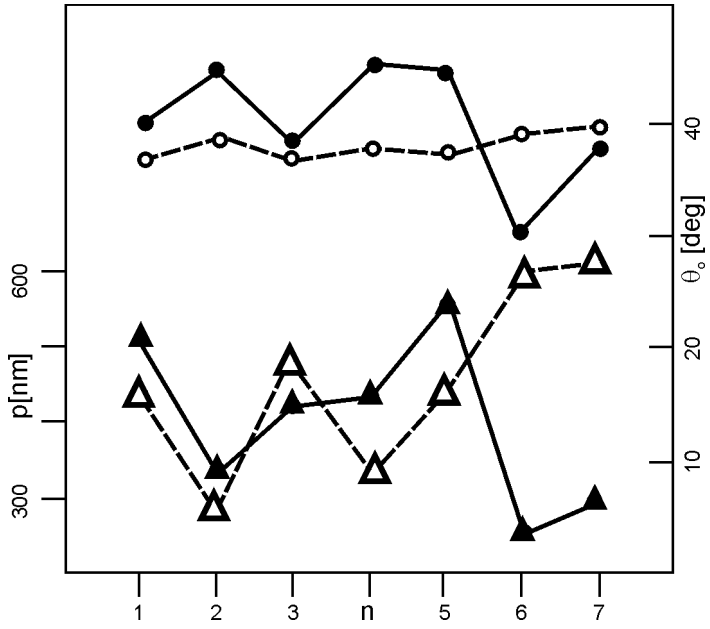

FIGURE 3 The comparisons of helical pitches p (▲- nF6B, △- nF6Bi) and optical tilt angles θ_o (●- nF6B, ○- nF6Bi) upon the number n of carbon atoms of fluorinated unit C_nF_{2n+1} for reduced temperature $T - T_{C_A-C} = -70\,K$.

the smectic layers (parallel to the helical axis) in the SmC^* or SmC_A^* phases, the part of helix which selectively reflects the light equals the half of the pitch. In this case

$$p = \lambda/\bar{n} \tag{5}$$

where $\bar{n}$ is the average refractive index (see chapter 2.4), and λ is the wavelength of a selective reflection band of AFLC.

The wavelength of a selective absorption band was measured by using a UV-VIS Varian Cary 3E spectrophotometer. The investigated compounds of nF6B homologous series were placed on the glass plate covered with a homeotropically aligning layer. The surface of the sample was left free. Results of the helical pitch measurements have been presented in the Figure 3.

It may be noted, that according to the theories given in [17–20] the helical pitch p increases almost proportionally to θ_o. As one can see in the Figure 3, the compounds with $n = 6$ and 7 for nF6B and with $n = 4,5,6,7$ for nF6Bi series satisfy these theories, while the remaining ones seem to show the opposite tendency.

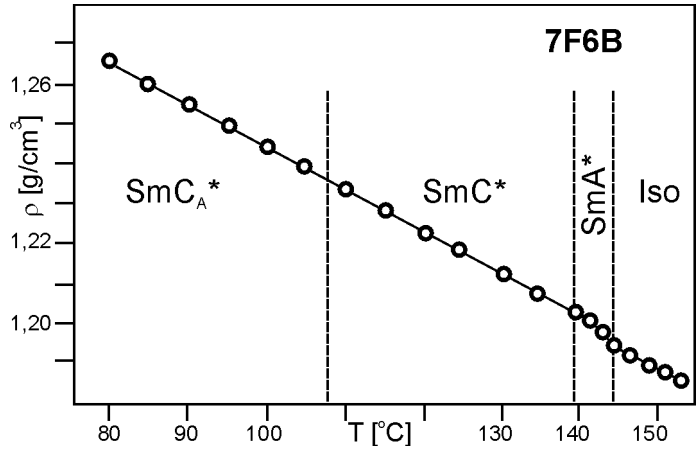

FIGURE 4 Temperature dependence of density ρ for Iso, SmA*, SmC* and SmC_A^* phases for 7F6B.

2.4. Density

The density ρ has been measured by means of the Anton Paar densitometer DMA46 with DMA 602 measuring cell in the Iso, SmA*, SmC* and SmC_A^* phases. Density ρ as a function of temperature for 7F6B compound is shown in Figure 4.

It is worth pointing out that density ρ of 7F6B remains continuous at the SmA* - SmC* and the SmC* – SmC_A^* transitions while the Iso – SmA* transition is accompanied by a slight decrease in the density as it is found for many liquid crystals with smectic phases.

2.5. Spontaneous Polarisation

Spontaneous polarisation P_S was measured by means of the Diamant bridge method and using a pulse technique. Both measurements were performed, using cells specially prepared. Results obtained from the Diamant bridge and pulse experiments agree with each other. Figures 5 and 6 show spontaneous polarisation and tilt angle for 2F6B and 7F6B versus temperature obtained in 2 μm cells with different boundary conditions and different measuring voltages.

The spontaneous polarisation P_S of tilted smectic layer in first approximation is directly proportional to molecular number density N, effective permanent dipole moment μ and tilt angle θ.

$$P_S \sim N\mu\theta \tag{6}$$

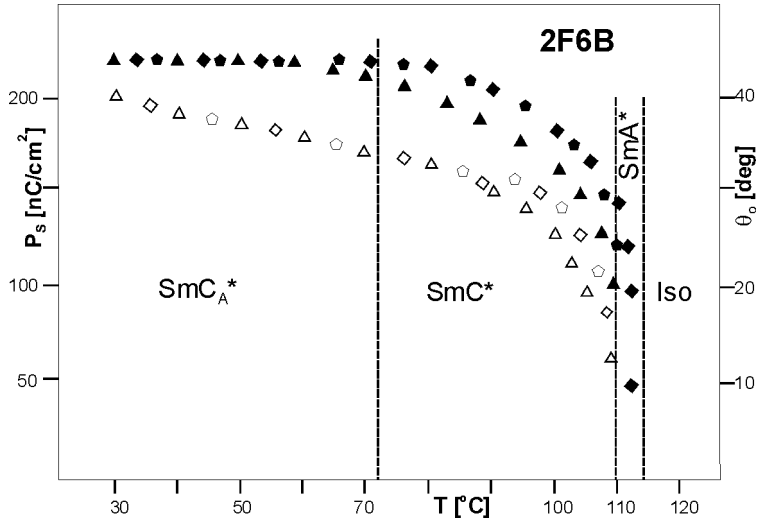

FIGURE 5 Spontaneous polarisation P_S and optical tilt angle θ_o of 2F6B as a function of temperature T: as for P_S – (△) nylon E = 5 V/μm, (⬠) polyimide E = 20 V/μm, (◇) polyimide E = 25 V/μm; as for θ_o – (▲) nylon E = 5 V/μm, (⬟) polyimide E = 20 V/μm, (◆) polyimide E = 25 V/μm.

According to (6), the spontaneous polarisation P_S should follow the tilt angle θ. One can see, that spontaneous polarisation P_S and the tilt angle θ_o of 7F6B under relatively "small" measuring electric field E (E = 5 V/μm) satisfy only the above statement (see Figure 6). When temperature characteristics of P_S and θ_o are saturated and they do not dependent on the magnitude of the electric filed E (for E > 20 V/μm and electrodes covered by polyimide) the shapes of P_S(T) for 2F6B and 7F6B do not fit the shapes of θ_o(T) curve.

The fact that the spontaneous polarisation P_s does not saturate with the temperature decrease for both mentioned AFLCs while the value of the tilt angle θ does saturate may be regarded as the evidence that the SmC* and SmC$_A$* phases are built up not only from monomers, but from dimers or even aggregates consisting of more than two molecules with partially antiparallel permanent dipole moments μ as well.

Some results obtained from dielectric measurements seem to confirm the suggestion that association processes appear in SmA*, SmC* and SmC$_A$* phases of 7F6B compound.

For the demonstration of dielectric properties of 2F6B the Cole–Cole plot in the SmA* phase has been shown in the Figure 7. One can see in this figure that relaxation mechanism in the SmA* phase of 2F6B can be described by two relaxation frequencies. Two

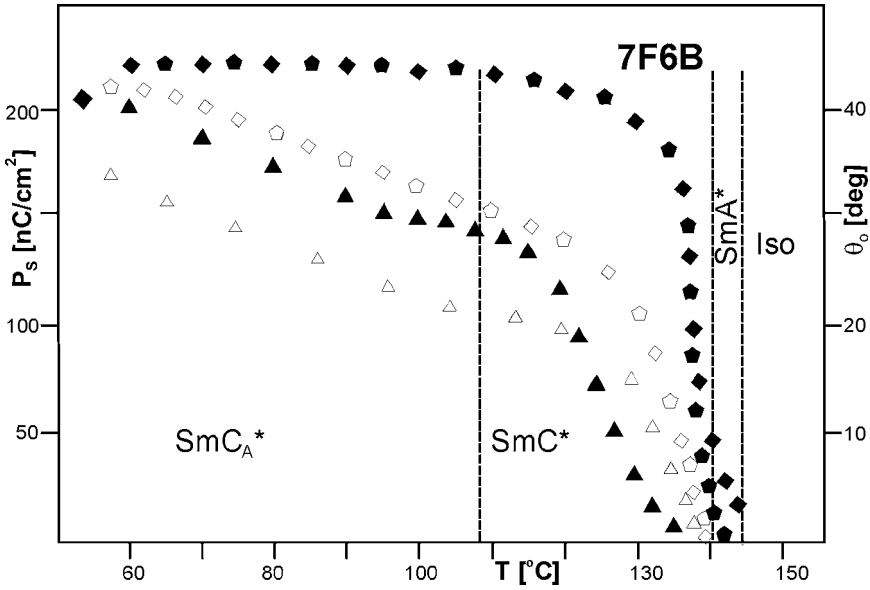

FIGURE 6 Spontaneous polarisation P_S and optical tilt angle θ_o of 7F6B as a function of temperature T: as for P_S – (△) nylon E = 5 V/μm, (⬠) polyimide E = 20 V/μm, (◇) polyimide E = 25 V/μm; as for θ_o – (▲) nylon E = 5 V/μm, (⬟) polyimide E = 20 V/μm, (◆) polyimide E = 25 V/μm.

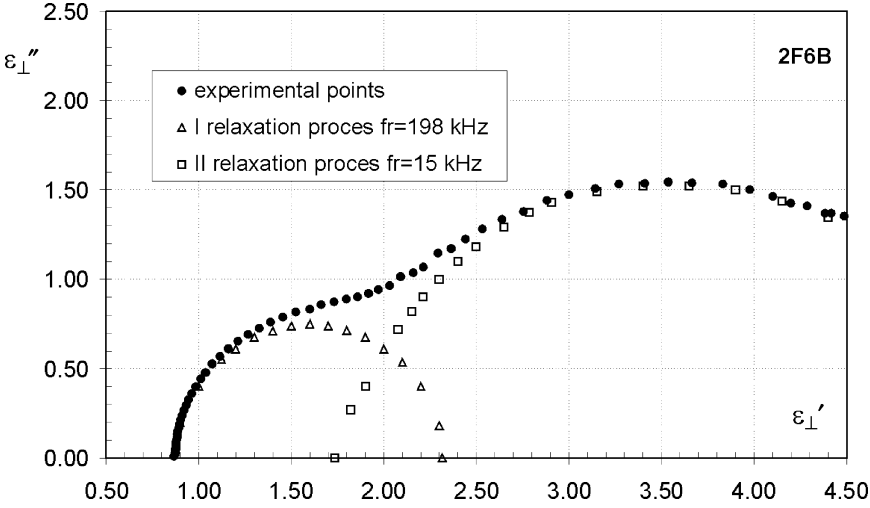

FIGURE 7 Cole–Cole plot for 2F6B in the SmA* phase.

frequencies $f_{r1} = 198\,kHz$ and $f_{r2} = 15\,kHz$ can be are probably connected with vibration of the molecules and their aggregates in the SmA* phase of 2F6B around the proper transverse axes of considered objects. Two types of relaxations described above were observed in the SmC* and SmC_A^* phases also.

2.6. Refractive Indices

The refractive indices: $n_i(T)$, $n_\perp(T)$ and $n_\parallel(T)$ in the Iso, SmA*, SmC* and SmC_A^* phases were measured using Abbe refractometer [21] with appropriate alignments.

The values of the $n_i(T)$, $n_\perp(T)$ and $n_\parallel(T)$ for 1F6B and 7F6B are presented graphically in Figures 8 and 9 respectively. Note that refractive indices $n_\perp(T)$ and $n_\parallel(T)$ shown in Figures 8 and 9 for the SmA*, SmC* and SmC_A^* phases are related to the optical axis perpendicular to the smectic layers. In the SmA* phase the axis mentioned above coincides with the molecular director **n** in smectic layers, while in the SmC* and SmC_A^* phases those directions are determined by the helical axes.

Investigated refractive indices $n_\perp(T)$ and $n_\parallel(T)$ are functions of the molecular polarizabillity (which can be regarded as constant in the

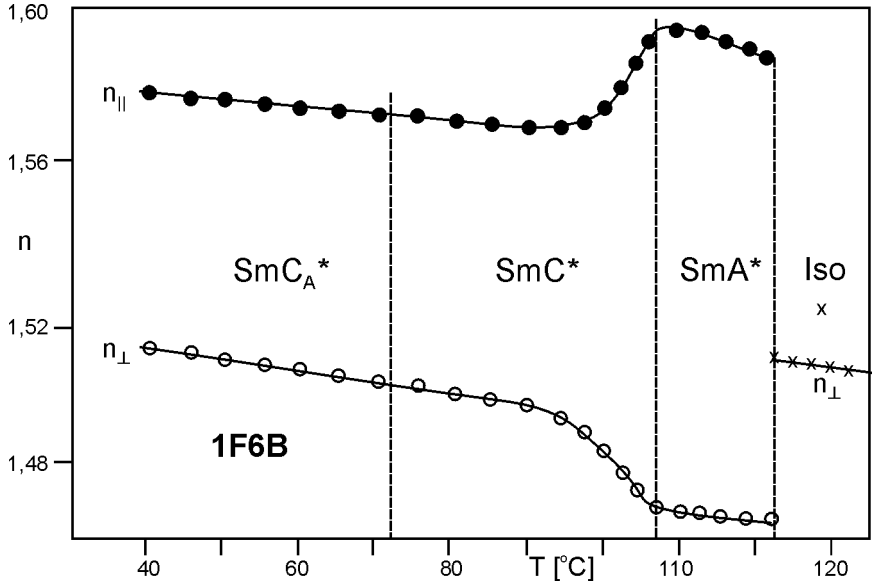

FIGURE 8 The refractive indices: $n_i(T)$, $n_\perp(T)$ and $n_\parallel(T)$ in the Iso, SmA*, SmC* and SmC_A^* for 1F6B.

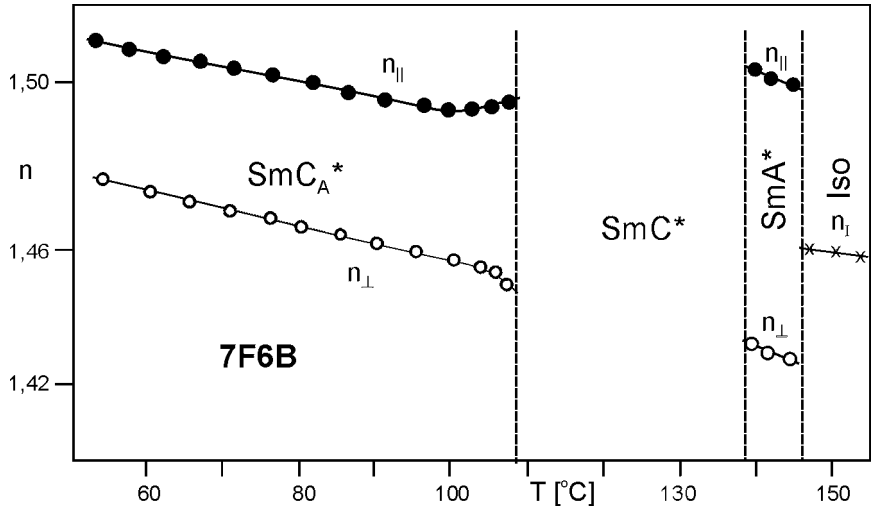

FIGURE 9 The refractive indices: $n_i(T)$, $n_\perp(T)$ and $n_{||}(T)$ in the Iso, SmA*, SmC* and SmC_A^* for 7F6B.

investigated temperature range), the molecular density number and molecular orientational order. Both the molecular density number (closely connected with density ρ) and molecular orientational order depend on temperature T.

Because molecular rotations around long molecular axes in the SmA*, SmC* and SmC_A^* phases are almost free (as was supposed in [21]), that any layer in para-, ferro- and antiferroelectric phases can be described by the same optical indicatrix. If we assume, that during the association process electron polarizabillity is additive, the shape of indicatrix will be the same but the directions of long (n_e) and short (n_o) axes will change from layer to layer in accordance with tilt θ_o and azimuthal Ω angles.

Knowing that for 7F6B in the SmC_A^* phase (with a helical structure) at 60°C $\theta_o = 45^\circ$ (see Fig. 6), $n_{||} = 1.52$ and $n_\perp = 1.47$ (see Fig. 9), one can calculate [22] that 7F6B indicatrix is characterised by $n_e = 1.63$ and $n_o = 1.43$ (see Fig. 10).

When one knows values of n_e and n_o of 7F6B indicatrix and temperature characteristics of $n_{||}(T)$, $n_\perp(T)$ and $\rho(T)$ in the SmA* phase, one can obtain an information about the structure of this phase. Our calculations have shown, that all the SmA* phases of nF6B compounds are de Vries-type phases [14,15]. It means that orthogonal layers are built from tilted domains. The distribution of the projection of the domain director on the plane of the smectic layer is random. In case

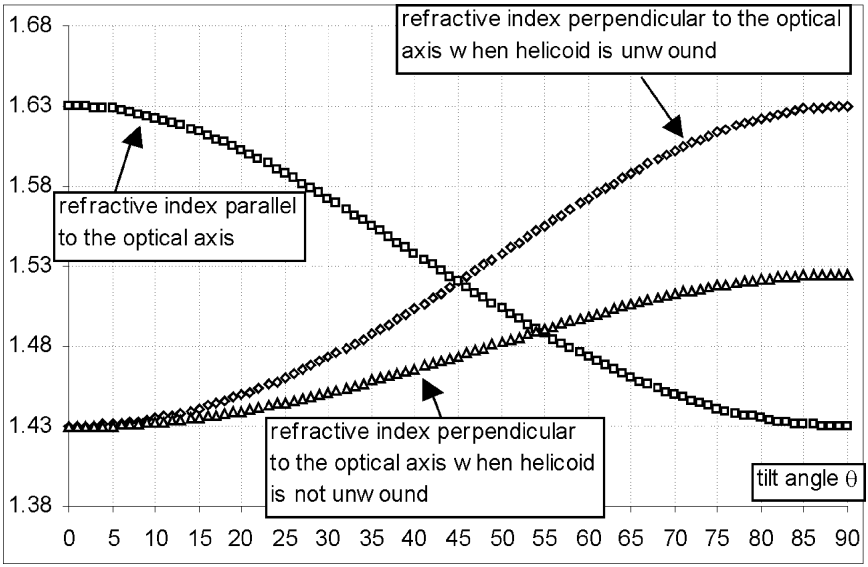

FIGURE 10 Computer calculation for refractive indices for unwound structure as well for helicoidal structure. For unwound structure both indices are identical for $\theta_o = 45^\circ$ (orthoconic case), whereas where helicoidal structure occurs, these indices are identical for higher tilt angle ($\theta_o = 54^\circ$); (calculations were made for $n_e = 1.63$ and $n_o = 1.43$). The long semi-axis is always parallel to the local molecular director. From relationship (given in [22]) between tilt angle θ_o(T) and refractive indices one can calculate tilt angles from refractive indices as well as refractive indices from tilt angle.

of 7F6B the tilt angle θ_A of de Vries cone is about 33° (see Fig. 10 when in the SmA* helicoid is unwound and $\Delta n = 0.70$) while for 1F6B in the SmA* phase $\theta_A = 25^\circ$ (see Fig. 10 when in the Sm A* phase $\Delta n = 0.13$).

It is worth underlining, that using the data gathered in Figure 10 it can be estimated that 1F6B in the SmC_A^* at 40°C ($\Delta n = 0.70$) should have θ_o about 40°, which agrees with our direct measurements (see Fig. 1).

2.7. Computer Simulation Results

To find shapes and functional dimensions of nF6B molecules Hyper Chem. 5.0 molecular modelling software with molecular mechanics method MM+ and semi-empirical method MNDO was used. In this way the optimum length l and the fully extended length l_m molecules were obtained. After this two molecules were put together in order to

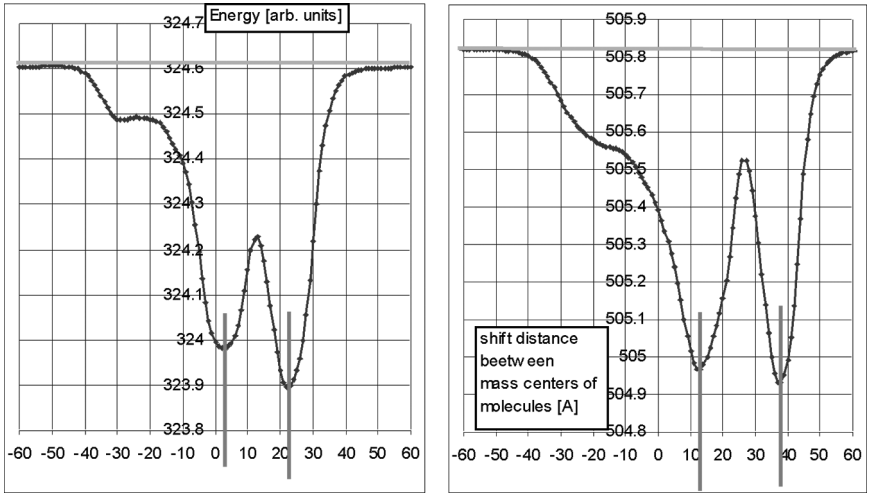

FIGURE 11 Interaction energy (using MM + molecular mechanics method) versus shift distance between mass centres of investigated molecules. Virtual dimers are built from two 7F6B molecules (right part of diagram) as well as from two 1F6B molecules (left part of diagram). Two minima are observed for antiparallel orientation.

estimate a virtual dimer. It was found out that there are two possible kinds of antiparallel dimers characterised by total length L_1 and L_2 (see Figures 11 and 12). The results of our computer simulations are partially shown in Table 2.

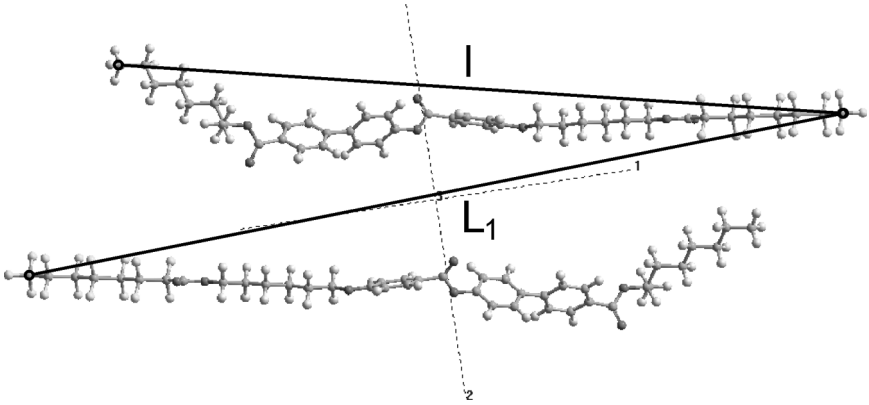

FIGURE 12 Virtual dimer built from two antiparallel 7F6B molecules. L_1 – denotes the total length of dimer in first energy minimum.

3. CONCLUSIONS

As described in chapter 2 experiments and computer calculations carried out on nF6B compounds give us some premises, that the uniaxial SmA^* phases of nF6B compounds and their phase transitions from the SmA^* to SmC^* phases follow the scheme proposed by de Vries [7,8,14,15]. (see Table 2)

Due to this model the objects from which the SmA^* phase is build up are tilted with respect to layer normal already in the SmA^* phase. In the simple rigid-rod approximations the average length L_A of these objects in the SmA^* phase (due to some association processes which produce dimers with $L_1 > l$ and $L_2 > l$) is higher then molecular length l. As a consequence of it, the tilt angle θ_A ($\theta_A = \text{acos}(d_A/L_A)$ in the d_A thick SmA^* layer is formed.

In such SmA^* layer the long axis of objects (molecules, dimers 1 and dimers 2) are randomly distributed on the surface of a cone centred around the layer normal. It is obvious that such arrangement produces uniaxial property of this phase. In our situation the SmA^*–SmC^* phase transition is found to have two aspects.

- Due to further association processes the number of dimers increases when temperature decreases and then the average length L (of objects from which the SmC^* phase is build) begin to be higher then L_A. So, the tilt angle θ ($\theta = \text{acos}(d/L)$ formed in the SmC^* layer with spacing d starts increasing at phase transition temperature $T_{A–C}$.
- Due to self organisation processes of new objects in new phase, the distribution of the long axis of these objects around the layer normal losses its rotational symmetry at phase transition temperature $T_{A–C}$. As a result, the formed a new SmC^* phase begin to have biaxial properties.

After comparison between the values of tilt angles θ obtained on the base of the above considerations with tilt angles θ_o, taken directly from electrooptical measurements ($\theta \sim \theta_o$), one can conclude that the origin of high optical tilt in fluorinated antiferroelectric liquid crystals is closely connected with some association processes which appear and raise their power when one goes from SmA^* through SmC^* to SmC_A^* phase. The high measured values of optical tilt θ_o ($\theta_o \approx 45^\circ$) in the SmC_A^* phase of nF6B compounds seems to be the result from the combination of rather high tilt θ_A ($\theta_A \approx 30^\circ$), which appears in the de Vries SmA^* phase) and an increase caused by compressing of layer spacing d in SmC_A^* and elongation of the length L of the objects which this phase built. Taking the above into account, in our opinion, the

suggestion about any influence the biasing rotation on the high tilt in the SmC_A^* phase of fluorinated antiferroelectrics [8,12] is generally true but plays a marginal role in this process.

REFERENCES

[1] Meyer, R. M., Liebert, L., Strzelecki, L., & Keller, P. (1975). *J. Phys. Lett*., *36*, L69.
[2] Chandani, A. D. L., Górecka, E., Ouchi, Y., Takezoe, H., & Fukuda, A. (1989). *Jap. J. Appl. Phys*., *28*, L1265.
[3] Lagerwall, S. T., Dahlgren, A., Jägemalm, P., Rudquist, P., D'havé, K., Pauwels, H., Dąbrowski, R., & Drzewiński, W. (2001). *Adv. Func. Mater*., *11*, 87.
[4] D'havé, K., Dahlgren, A., Rudquist, P., Lagerwall, J. P. F., Andersson, G., Matuszczyk, M., Lagerwall, S. T., Dąbrowski, R., & Drzewiński, W. (2000). *Ferroelectrics*, *244*, 115.
[5] D'havé, K., Rudquist, P., Lagerwall, S. T., Pauwels, H., Drzewiński, W., & Dąbrowski, R. (2000). *Appl. Phys. Let*., *76*, 3528.
[6] Drzewiński, W., Czupryński, K., Dąbrowski, R., Raszewski, Z., Rutkowska, J., Górecka, E., & Neubert, M. (1998). *SPIE Proc*., 3319, 100.
[7] Lagerwall, J. P. F., Giesselman, F., & Radcliffe, M. D. (2002). *Phys. Rev. E*, *66*, 031703.
[8] Lagerwall, J. P. F., Saipa, A., Giesselman, F., & Dąbrowski, R. private announcement,
[9] Dąbrowski, R., Gąsowska, J., Otón, J., Piecek, W., Przedmojski, J., & Tykarska, M. (2004). *Displays*, *25*, 1.
[10] Gąsowska, J., Dąbrowski, R., Drzewiński, W., Filipowicz, M., Przedmojski, J., & Kenig, K., (FLC'03, Dublin), (2004) *Ferroelectrics, 309*, 83.
[11] Gąsowska, J., Dziaduszek, J., Drzewiński, W., Filipowicz, M., Dąbrowski, R., Przedmojski, J., & Kenig, K., (CLC'03, Zakopane), (2004) *SPIE Proceedings, 5565*, 72.
[12] Piecek, W., Raszewski, Z., Perkowski, P., Przedmojski, J., Kędzierski, J., Drzewiński, W., Dąbrowski, R., & Zieliński, J., (FLC'03, Dublin), (2004) *Ferroelectrics, 310*, 269.
[13] Beccherelli, R. R. & Elson, S. J. (1998). *Liq. Cryst*., *25*, 573.
[14] de Vries, A. (1979). *J. Chem. Phys*., *71*, 25.
[15] de Vries, A., Ekachai, A., & Spielberg, N. (1979). *Mol. Cryst. Liq. Cryst. Lett*., *49*, 143.
[16] Raszewski, Z., Kędzierski, J., Rutkowska, J., Piecek, W., Perkowski, P., Czupryński, K., Dąbrowski, R., Drzewiński, W., Zieliński, J., & Żmija, J. (2001). *Mol. Cryst. Liq. Cryst*., *366*, 607.
[17] Blinc, R., Žeks, B., Musevic, J., & Levstic, A. (1984). *Mol. Cryst. Liq. Cryst*., *114*, 189.
[18] Nakagawa, M. (1988). *Liq. Cryst. Lett*., *3*, 573.
[19] Yamashita, M. & Kimura, H. (1982). *J. Phys. Soc. Jap*., *51*, 2419.
[20] Ji Li, Takezoe, H., & Fukuda, A. (1991). *Jap. J. Appl. Phys*., *30*, 532.
[21] Raszewski, Z., Kędzierski, J., Perkowski, P., Piecek, W., Rutkowska, J., Kłosowicz, S., & Zieliński, J. (2003). *Ferroelectrics*, *276*, 289.
[22] Perkowski, P., Raszewski Z., Kędzierski, J., Piecek, W., Rutkowska, J., Zieliński, J., Dąbrowski, R., Drzewiński, W., (FLC'03, Dublin), will be published in Ferroelectrics.